The N-terminus of the human copper transporter 1 (hCTR1) is localized extracellularly, and interacts with itself

Adriana E. M. KLOMP, Jenneke A. JUIJN, Linda T. M. VAN DER GUN, Inge E. T. VAN DEN BERG, Ruud BERGER and Leo W. J. KLOMP[1]

Department of Metabolic and Endocrine Diseases, University Medical Center Utrecht, Room KC.02.069.1, Lundlaan 6, 3584 EA Utrecht, The Netherlands

We have used indirect immunofluorescense studies and glycosylation-site insertion and deletion mapping to characterize the topology of human copper transporter 1 (hCTR1), the putative human high-affinity copper-import protein. Both approaches indicated that hCTR1 contains three transmembrane domains and that the N-terminus of hCTR1, which contains several putative copper-binding sites, is localized extracellularly, whereas the C-terminus is exposed to the cytosol. Based on previous observations that CTR1 proteins form high-molecular-mass complexes, we investigated directly whether CTR1 proteins interact with themselves. Yeast two-hybrid studies showed that interaction of yeast, mouse, rat and human CTR1 occurs at the sites of their N-terminal domains, and is not dependent on the copper concentration in the growth media. Analysis of deletion constructs indicated that multiple regions in the N-terminus are essential for this self-interaction. In contrast, the N-terminal tail of the presumed low-affinity copper transporter, hCTR2, does not interact with itself. Taken together, these results suggest that CTR1 spans the membrane at least six times, permitting formation of a channel, which is consistent with its proposed role as a copper transporter.

Key words: copper transport, membrane topology, N-linked glycosylation, oligomerization, solute carrier.

INTRODUCTION

Copper is an essential nutrient for life. Due to its ability to exist in two oxidation states, copper is an important redox cofactor for many copper-dependent enzymes, including cytochrome c oxidase, ceruloplasmin, copper/zinc superoxide dismutase and lysyl oxidase [1,2]. The redox property that makes copper an essential element of biological systems also makes it toxic. Redox cycling between Cu(II) and Cu(I) can catalyse the production of highly toxic hydroxyl radicals, with subsequent damage to lipids, proteins and DNA [3]. It is therefore of great importance to control cellular copper content. Work in yeast, plants, mice and humans has resulted in a model of intracellular copper-trafficking pathways [4,5].

In *Saccharomyces cerevisiae*, copper import is mediated by a low-affinity copper transporter protein yCtr2p, and by two high-affinity copper transporters, yCtr1p and yCtr3p [6,7]. The yeast Ctr1 protein, which is extensively modified by the addition of O-linked oligosaccharides, is localized at the plasma membrane [8,9]. Upon high extracellular copper concentrations, yCtr1p is endocytosed and degraded; the latter process is dependent on expression of the transcription factor Mac1p [9,10]. Copper transporter (CTR) 1 protein of other species, including mammals, can complement the growth phenotypes of yeast cells which are, due to inactivation of both the *yCtr1* and *yCtr3* genes, defective in copper transport [11]. Human CTR (hCTR) 2 is structurally similar to hCTR1, but fails to complement the growth phenotype of yCtr1/yCtr3-deficient yeast. It was therefore proposed that hCTR2 represents a low-affinity copper-import protein [11].

The *hCTR1* gene encodes a protein of 190 amino acids. Biosynthetic studies revealed that hCTR1 is synthesized as a precursor protein of 28 kDa containing N-linked oligosaccharides, and is converted to a mature protein of approx. 35 kDa, which is expressed ubiquitously [12]. Between different cell types subcellular hCTR1 localization differed markedly, from an intracellular vesicular perinuclear compartment in HeLa cells, to the plasma membrane in Caco2 cells. This steady-state localization seems to be the result of a dynamic process, which involves constitutive endocytosis of hCTR1 from the plasma membrane [12]. In contrast to yCtr1p, the localization of hCTR1 is not influenced by copper concentrations [8,9,12]. There are some indications that exogenous epitope-tagged hCTR1 associates with higher-molecular-mass protein complexes [13]. Exogenously epitope-tagged yCtr1p exists as an oligomer *in vivo* [8].

Recent observations provide support for an important physiological role of CTR1 proteins in copper acquisition in mammalian cells. Immortalized cells transfected with cDNA constructs encoding epitope-tagged hCTR1 or murine CTR1 accumulate excess ^{64}Cu, with a K_m of 1–5 μM [14–16]. The crucial role for CTR1 in embryogenesis is demonstrated by mice with a homozygous disruption at the murine *CTR1* locus, resulting in severe developmental defects and death *in utero*, presumably as a consequence of copper deficiency [14,17].

Similar to the *S. cerevisiae* Ctr1 and Ctr3 proteins, analysis of the amino acid sequence of hCTR1 predicts the presence of two hydrophobic stretches, whereby the second hydrophobic region consists of 40 amino acids, and thus could encompass either one or two transmembrane domains [11]. To characterize the membrane topology of hCTR1, confocal fluorescence microscopy techniques and an N-linked glycosylation mapping strategy were employed. Further, the impact of N-linked glycosylation on hCTR1 protein synthesis and localization was investigated. Finally, based on previous work [13], we hypothesized that hCTR1 interacts with itself and used the yeast two-hybrid system to test this hypothesis. Our results are integrated in a model describing the topology of hCTR1.

Abbreviations used: BCS, bathocuproine disulphonic acid; CTR, copper transporter; ER, endoplasmic reticulum; hCTR, human CTR; ONPG, *o*-nitrophenyl-β-D-galactopyranoside; VSV-G, vesicular stomatitis virus-G protein.

[1] To whom correspondence should be addressed (e-mail L.Klomp@azu.nl).

EXPERIMENTAL

Materials

Oligonucleotides were purchased from Isogen Bioscience (Maarssen, The Netherlands). Hybridoma clone P5D4 [anti-vesicular stomatitis virus-G protein (anti-VSV-G)] was kindly provided by Dr J. Fransen (Department of Cell Biology, University of Nijmegen, Nijmegen, The Netherlands). Antibodies used for immunofluorescence studies were as follows: anti-TGN p230 (BD Biosciences, San Jose, CA, U.S.A.), and Cy3™- or FITC-conjugated affiniPure donkey anti-mouse or anti-rabbit IgG (H+L; Jackson ImmunoResearch Laboratories, West Grove, PA, U.S.A.). Generation of polyclonal rabbit antiserum raised against a recombinant fusion protein encoding the N-terminal part of hCTR1 fused to six histidine residues is described elsewhere [12].

Plasmid constructs

Construction of pZeoSV2 expressing 3′ VSV-G-tagged hCTR1 (hCTR1-VSV-G) was described previously [12]. Mutations were engineered by oligonucleotide-directed mutagenesis kit (Stratagene, Cedar Creek, TX, U.S.A.) using oligonucleotides F1 and R1 (hCTR1-N15D), F2 and R2 (hCTR1-N112D) and F3 and R3 (hCTR1-D184N), respectively (Table 1 shows the oligonucleotides used in this study) [11]. A plasmid encoding 3′ VSV-G-tagged hCTR1, lacking its third putative transmembrane domain (bp 481–525; amino acids 160–175), was constructed in three steps. First, a 3′ VSV-G-tagged part of hCTR1 (bp 526–573) was amplified by PCR using specific oligonucleotides containing either a *Kpn*I (F4) or a *Xho*I (R4) restriction site added to their 5′ ends. As templates, plasmids encoding wild-type or mutated VSV-G-tagged hCTR1 were used. Secondly, the remaining 5′ part of hCTR1 (bp 1–480) was isolated from pZeoSV2 encoding 3′ VSV-G-tagged full-length hCTR1, by digestion with *Bam*HI and *Kpn*I. The two fragments were ligated in pZeoSV2, which was predigested with *Bam*HI and *Xho*I. The correct open reading frame was confirmed by direct sequencing.

To generate plasmids for the yeast two-hybrid interaction analyses, the different domains of hCTR1 were amplified by PCR using specific oligonucleotides containing either a *Sma*I or a *Sal*I restriction site added to their 5′ ends. For amplification of cDNA encoding amino acids 1–70 of hCTR1, primers F5 and R5 were used; for amino acids 1–39, primers F5 and R13; for amino acids 18–70, primers F14 and R5; for amino acids 40–70, primers F15 and R5; for amino acids 84–135, primers F6 and R6; and for amino acids 173–190, primers F7 and R7. For amplification of cDNA encoding the N-termini of murine CTR1 (amino acids 1–68) [18], rat CTR1 (amino acids 1–67; GenBank accession number AF26 58030), yeast CTR1 (amino acids 1–154) [6] and human CTR2 (amino acids 1–22) [11], we used primers F8 and R8, F9 and R8, F10 and R9, and F11 and R10 respectively. Full-length hATOX1 [19] was amplified using oligonucleotides F12 and R11, and the first four metal-binding motifs of ATP7B (amino acids 45–440) [20] were amplified with F13 and R12. The fragments were ligated in the *Sma*I and *Sal*I sites of pGBT9 and pGADGH, and the correct open reading frames were confirmed by direct sequencing. The N-terminal part of yCtr1 was cloned into the *Sma*I and *Bam*HI sites of pGBT9, or the *Sma*I and *Xho*I sites of pGADGH, respectively. Plasmids pGBT9 and pGADGH were kindly given by Dr J. Leusen (Immunotherapy Laboratory, University Medical Center Utrecht, Utrecht, The Netherlands), and were originally from BD Biosciences Clontech (Palo Alto, CA, U.S.A.).

Table 1 Oligonucleotides used in this study for cloning and mutagenesis

Primers are depicted 5′ → 3′. Introduced restriction sites are underlined.

Primer name	Nucleotide sequence
F1	GAG CTA TAT GGA CTC CGA CAG TAC CAT GCA ACC
F2	CCT GTC CCA GGA CCA GAT GGA ACC ATC CTT ATG G
F3	GAA GAA GGC AGT GGT AGT GAA TAT CAC AGA GCA TTG CC
F4	GGG TAC CTC AGC TGG AAG AAG GCA GTG
F5	T CCC CCG GGA ATG GAT CAT TCC CAC CAT ATG GG
F6	C CCG GGT GAA GGA CTC AAG ATA GCC
F7	T CCC CCG GGC TTC CTC TTC AGC TGG AAG
F8	C CCG GGT ATG AAC CAT ATG GGG ATG AAC
F9	C CCG GGT ATG AGG ATG AAC CAC ATG GAG
F10	C CCG GGA ATG GAA GGT ATG AAT ATG GG
F11	T CCC CCG GGC ACC ATG GCG ATG CAT TTC A
F12	T CCC CCG GGC ATG CCG AAG CAC GAG TTC TC
F13	T CCC CCG GGT GAA GGT GGT CTG GAT GGC C
F14	C CCG GGC ATG CAA CCT TCT CAC CAT C
F15	C CCG GGC ATG ATG ATG ATG CCT ATG AC
R1	GGT TGC ATG GTA CTG TCG GAG TCC ATA TAG CTC
R2	CCA TAA GGA TGG TTC CAT CTG GTC CTG GGA CAG G
R3	GGC AAT GCT CTG TGA TAT TCA CTA CCA CTG CCT TCT TC
R4	CTC GAG TCA CTT TCC TAG TCG GTT CAT
R5	A CGC GTC GAC AGC CAT TTC TCC AGC TGT ATT GA
R6	GTC GAC TTG CAG GAG GTG AGG AAA
R7	A CGC GTC GAC TCA ATG GCA ATG CTC TGT GAT
R8	GTC GAC CTA AGC CAT TTC TCC AGG TGT
R9	GTC GAC CTA GAA AGC CTT ACC ACT ATT G
R10	GTC GAC CTA ACT GTG GAC ACT CCA GAA ATC
R11	ACG CGT CGA CTG CTA CTC AAG GCC AAG GTA
R12	ACG CGT CGA CGC ACT GTG GTT TCC AAG AGG
R13	GTC GAC CTA GCT GCT GTC TCC TCC ACC

Cell culture and transient transfection

Cell lines were purchased from the American Type Culture Collection (Rockville, MD, U.S.A.). Culture media and solutions were purchased from Life Technologies (Breda, The Netherlands). Cells were cultured at 37 °C under humidified air containing 5% CO_2, and according to the manufacturer's instructions. Transient transfections were performed using LipofectAMINE 2000 (Life Technologies) according to the manufacturer's instructions.

Biosynthetic labelling and immunoprecipitation

Biosynthetic labelling, using [^{35}S]methionine and [^{35}S]cysteine, of proteins in cell lines, and immunoprecipitation were performed as described in [12]. Tunicamycin was purchased from Roche (Basel, Switzerland).

Confocal immunofluorescence microscopy

The cells were seeded and grown on cover slips (Marienfeld, Paul GmbH & Co. KG, Bad Mergentheim, Germany). Immunofluorescence studies on fixed cells were performed as described in [12]. For live-cell immunofluorescence under non-permeabilized conditions, staining was performed at 4 °C. Cells were washed with PBS, blocked by incubation with 5% BSA in PBS for 1 h, incubated with primary antibodies for 2 h, washed and fixed with 4% paraformaldehyde in PBS for 20 min. After a final wash in PBS proteins were visualized by incubation for 1 h with fluorescent secondary antibodies. Confocal light-microscopy analysis

was performed on a Leica TCS 4D microscope using dedicated image software.

Yeast two-hybrid studies

Yeast culture media and solutions were purchased from BD Diagnostic Systems (Sparks, MD, U.S.A.). The yeast two-hybrid assay was performed according to the protocol supplied by the yeast two-hybrid system supplier (BD Biosciences Clontech). Activation of the HIS3 reporter gene was tested by growing transformed yeast strains on plates lacking leucine, tryptophan and histidine, and containing 5 mM 3-amino-1,2,4-triazole. To test the copper-dependence of interactions, transformed yeast strains were grown in the presence of 3 mM bathocuproine disulphonic acid (BCS) for 24 h in synthetic drop-out medium lacking leucine, tryptophan and histidine. The interactions were then quantified by a liquid culture assay using *o*-nitrophenyl-β-D-galactopyranoside (ONPG) as a substrate, as described by others [21].

RESULTS

Probing hCTR1 topology by epitope accessibility and indirect immunofluorescence

Hydropathy analysis of the primary sequence of hCTR1 using the Kyte–Doolittle algorithm [22] predicts the presence of two hydrophobic regions (amino acids 68–86 and 133–173). Predictive algorithms can sometimes incorrectly assign the topology of proteins [23]. Therefore, indirect immunofluorescence studies were performed to determine the localization of the N- and C-termini of hCTR1. We used Caco2 and HeLa cells, since we have previously shown hCTR1 plasma membrane staining in both cell lines [12]. When immunofluorescence studies using antiserum raised against the N-terminus of hCTR1 were performed in the absence of Triton X-100, in both cell lines hCTR1 staining was clearly detectable at the plasma membrane (Figure 1A). No intracellular staining of *trans*-Golgi-network marker p230 was detected, indicating that cells were indeed not permeabilized. In the presence of Triton X-100 we clearly detected intracellular p230 staining (results not shown) [12].

To determine the localization of the C-terminus of hCTR1, H441 cells were transiently transfected with a construct encoding hCTR1 with a C-terminal VSV-G tag. Previously, we have shown that exogenous VSV-G-tagged hCTR1 is a stable protein with the appropriate molecular mass [12]. Exogenous hCTR1 was stained with anti-VSV-G antibody. Transfected cells clearly showed marked overexpression of hCTR1. In permeabilized cells staining patterns of anti-hCTR1 and anti-VSV-G overlapped (Figure 1B). In non-permeabilized cells, antiserum raised against the N-terminus of hCTR1 showed overexpression of hCTR1 at the plasma membrane in approx. 5% of the cells, indicating that these were transfected cells. In the same cells no staining was detected with anti-VSV-G antibody, indicating that the epitope for this antibody was localized in the cytoplasm of the cell. Taken together, these data indicate that the N-terminus of hCTR1 is localized extracellularly, whereas the C-terminus is exposed to the cytosol. This implies that hCTR1 contains three transmembrane domains, and that the second hydrophobic region encompasses two transmembrane domains.

Probing hCTR1 topology by N-linked glycosylation mapping

Sequence analysis of hCTR1 shows that hCTR1 has two potential N-linked glycosylation consensus sites (Asn-Xaa-Ser/Thr), which are separated by the first hydrophobic stretch of amino

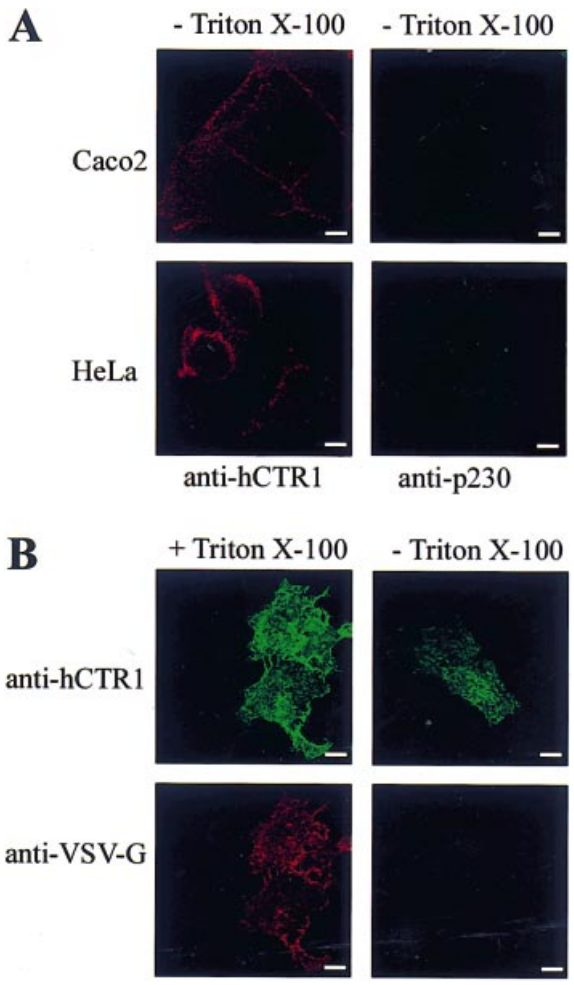

Figure 1 Elucidation of hCTR1 topology by indirect immunofluorescence

(**A**) Localization of the N-terminus of hCTR1. Caco2 cells or HeLa cells were analysed by double-label indirect confocal immunofluorescence, in the absence of Triton X-100 using a polyclonal rabbit antiserum raised against a recombinant fusion protein encoding the N-terminal part of hCTR1 fused to six histidines [12], followed by Cy3-conjugated donkey anti-rabbit IgG, and anti-p230 visualized with FITC-conjugated donkey anti-mouse IgG. (**B**) Localization of the C-terminus of hCTR1. H441 cells transfected with a construct encoding hCTR1 containing a C-terminal VSV-G tag, were analysed by double-label indirect immunofluorescence, in the presence or absence of Triton X-100 using anti-hCTR1 and anti-VSV-G, visualized with FITC-conjugated donkey anti-rabbit IgG and Cy3-conjugated donkey anti-mouse IgG, respectively. Scale bars, 10 μm.

acids (residues 68–86), suggesting that only one site is projected into the endoplasmic reticulum (ER) lumen, and is therefore substituted. Previously we have shown that hCTR1 is modified by N-linked glycosylation [12]. To test which of the putative sites are N-glycosylated *in vivo*, we engineered two mutant constructs in which aspartate residues replaced each of the consensus asparagines (Figure 2, constructs hCTR1-N15D and hCTR1-N112D). Further, a construct with a novel consensus N-linked glycosylation site (Figure 2, NXT) at the C-terminal tail of hCTR1, after the second hydrophobic region (amino acids 133–173), was generated by changing the aspartate at postition 184 to an asparagine (Figure 2, construct hCTR1-D184N). The cDNAs encoding these mutant hCTR1 proteins were then expressed in H441 cells, and 24 h after transfection cells were metabolically labelled for 2 h, lysed and used for immunoprecipitation with anti-VSV-G antibody. Analysis of expressed

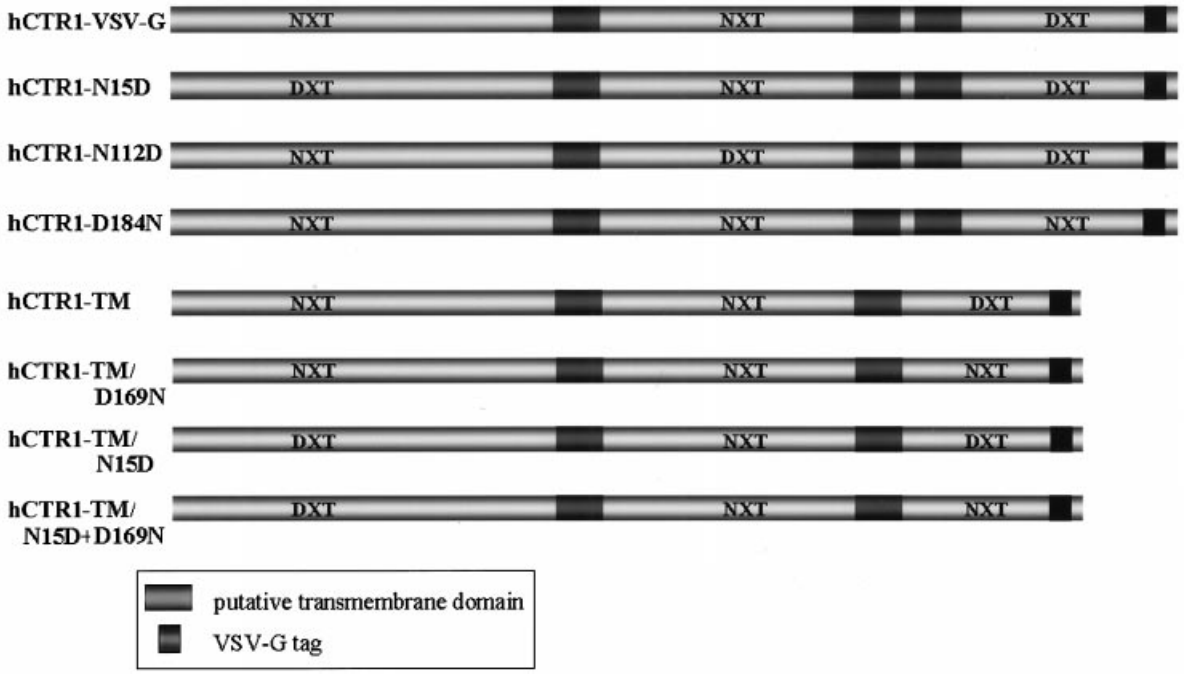

Figure 2 Constructs used for glycosylation mapping

Schematic representation of constructs encoding VSV-G-tagged hCTR1. Putative transmembrane domains are indicated by dark-grey boxes, the C-terminal VSV-G-tag is represented by a black box. Amino acid substitutions to either change asparagine residues (N15D and N112D), thus removing putative consensus N-linked glycosylation sites, or replace aspartate residues with asparagine (D184N and D169N), thus creating N-linked glycosylation sites, are marked. Constructs with a deletion of the third putative transmembrane domain (amino acids 160–175) are named 'hCTR1-TM'. NXT and DXT represent one-letter amino acid code.

proteins indicated that mutation N15D caused a marked reduction in apparent molecular mass of immunoprecipitated VSV-G-tagged hCTR1 (Figure 3A). Mutations N112D and D184N had no effect on the apparent molecular masses of the detected proteins.

To confirm that this decrease in apparent molecular mass of mutant N15D is due to the absence of N-linked glycosylation, transiently transfected cells were preincubated for 4 h with tunicamycin, an inhibitor of N-glycosylation [24], followed by a 10 min pulse and a 90 min chase in the presence of tunicamycin, and immunoprecipitation of VSV-G-tagged hCTR1. When cells were transiently transfected with hCTR1-VSV-G, hCTR1-N112D and hCTR1-D184N, precursors of 28 kDa and mature hCTR1 of 35 kDa were detected as shown previously [12]. The apparent molecular masses of these polypeptides decreased as a result of prior tunicamycin treatment (Figure 3B, upper left-hand and lower left- and right-hand panels), indicating that the proteins were substituted with N-linked oligosaccharides. When cells were transfected with hCTR1-N15D, smaller-sized precursor and mature hCTR1 proteins were detected (Figure 3B, upper right-hand panel). Tunicamycin treatment had no effect on SDS/PAGE mobility of hCTR1-N15D, strongly suggesting that these proteins did not contain N-linked oligosaccharides.

For the glycosylation mapping assay described above, we left the two natural consensus glycosylation sites of hCTR1 intact and introduced a new glycosylation acceptor site at a position close to a putative transmembrane domain. This introduced N-linked glycosylation site was not modified *in vivo* (Figure 3A and the lower right-hand panel of Figure 3B). This indicates that the site was exposed to the cytosol, or that the engineered consensus glycosylation acceptor site had passed through the ER lumen, but was somehow not substituted. Consistent with the latter possibility, a consensus glycosylation site can only be modified by oligosaccharyltransferase if this site is placed at a 'precise minimal glycosylation distance' from a transmembrane segment [25]. To test whether the C-terminal introduced N-linked glycosylation site can be substituted *in vivo*, constructs encoding truncated forms of hCTR1, lacking the last 15 amino acids of the second hydrophobic region, were generated (Figure 2, constructs hCTR1-TM, hCTR1-TM/D169N, hCTR1-TM/N15D and hCTR1-TM/N15D+D169N). Analysis of expressed proteins showed that truncated VSV-G-tagged hCTR1 had a decreased apparent molecular mass compared with full-length VSV-G-tagged hCTR1 (compare lanes 1 in Figures 3C and 3A). Introduction of mutation D169N in the construct encoding the truncated protein, corresponding to D184N in full-length hCTR1, caused an increase in the apparent size (Figure 3C), indicating that this site was indeed used as an N-linked glycosylation site *in vivo*. When the N15D mutation was introduced instead of D169N, thereby knocking out a consensus N-linked glycosylation site, the detected truncated protein had a decreased apparent molecular mass compared with non-mutated truncated VSV-G-tagged hCTR1. A construct containing both N15D and D169N mutations encoded a truncated protein with the same electrophoretic mobility as non-mutated truncated VSV-G-tagged hCTR1. Therefore, the engineered aspartate at position 184 in the full-length hCTR1 can be substituted by N-linked glycosylation, but only when removal of the last transmembrane region causes it to project into the ER lumen.

Taken together, these data directly demonstrate that the C-terminal tail of hCTR1, and the loop of hCTR1 between the two hydrophobic stretches, are localized in the cytosol. The N-

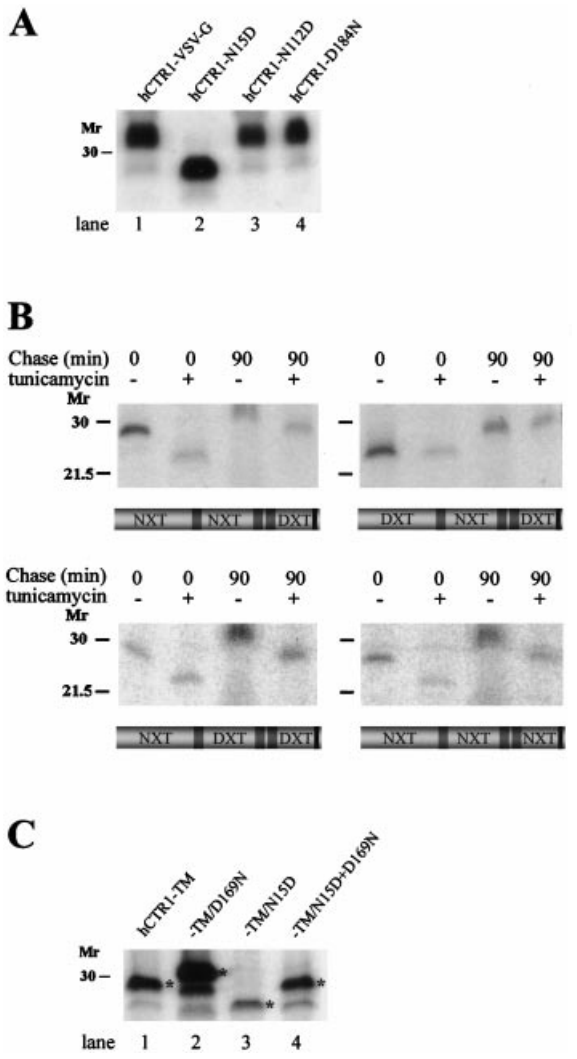

Figure 3 Elucidation of hCTR1 topology by glycosylation mapping

(**A**) H441 cells were transiently transfected with VSV-G-tagged hCTR1 containing no mutations (hCTR1-VSV-G; lane 1), or mutations N15D (lane 2), N112D (lane 3) or D184N (lane 4). Cells were labelled with Tran[^{35}S]^{TM} for 2 h and immunoprecipitation was performed with anti-VSV-G. Proteins were separated by SDS/PAGE and analysed by fluorography. (**B**) H441 cells, transfected with the schematically indicated constructs, were preincubated with or without tunicamycin for 4 h, pulse-labelled with Tran[^{35}S]^{TM} for 10 min and chased for the indicated time periods with unlabelled methionine. hCTR1 proteins were isolated and analysed as in (**A**). (**C**) H441 cells were transfected with constructs encoding VSV-G-tagged hCTR1 lacking its third putative transmembrane domain, either containing no mutations, mutation N15D, mutation D169N or both. hCTR1 proteins were isolated and analysed as in (**A**). Mature hCTR1 proteins are indicated by asterisks, lower-molecular-mass polypeptides represent biosynthetic intermediates. Molecular-mass markers are indicated on the left. NXT and DXT represent one-letter amino acid code.

terminus of hCTR1 has passed through the ER lumen, and is therefore localized extracellularly. We can also conclude that N15 is the sole N-linked glycosylation site within hCTR1 that is used *in vivo*.

Effect of mutation N15D on hCTR1 biosynthesis and localization

To investigate whether the N-linked oligosaccharide chain at position N15 is required for maintaining the biochemical characteristics of wild-type hCTR1, the effect of knocking out this N-linked glycosylation site was studied. Pulse-chase experiments were performed to investigate the effect of the N15D mutation on hCTR1 protein synthesis. H441 cells were transiently transfected with constructs encoding either wild-type or mutant N15D VSV-G-tagged hCTR1. After 24 h, cells were pulse-labelled with Tran[^{35}S]^{TM} for 10 min and subsequently chased for different time periods. Immunoprecipitation was performed with anti-VSV-G antibody. Figure 4(A) shows that wild-type VSV-G-tagged hCTR1 was synthesized as a precursor of 28 kDa, which was converted to a mature protein of 35 kDa within 45 min. VSV-G-tagged hCTR1 containing mutation N15D matured faster from a precursor of 23 kDa to a mature protein of 30 kDa. No marked difference was detectable between the half-life times of the two mature VSV-G-tagged hCTR1 proteins (results not shown), suggesting that the stability of both proteins was comparable.

To determine the influence of the N-linked oligosaccharide chain on subcellular localization of hCTR1, double-label indirect immunofluorescence was performed on transiently transfected H441 cells. Endogenous and exogenous hCTR1 was stained with anti-hCTR1 and the *trans*-Golgi network was stained with anti-p230. Endogenous hCTR1 was localized in a vesicular intracellular compartment that was situated in close proximity to the *trans*-Golgi network marker as well as at the plasma membrane. Cells transfected with a construct encoding wild-type VSV-G-tagged hCTR1, showed hCTR1 staining on the plasma-membrane, but also some staining in intracellular vesicular structures (Figure 4B). Cells transfected with a construct containing mutation N15D showed the same staining pattern, indicating that loss of the N-linked glycosylation had no detectable influence on subcellular localization.

Next, immunofluorescence studies on non-permeabilized transfected cells were performed to determine whether the hCTR1 mutant lacking the N-linked glycan was localized at the plasma-membrane. In cells transfected either with mutant or wild-type hCTR1, hCTR1 staining was clearly detectable at the plasma-membrane (Figure 4C). No intracellular staining of *trans*-Golgi-network marker p230 was detected, indicating that cells were not permeabilized.

Interaction of hCTR1 with itself

Exogenous epitope-tagged hCTR1 and yCtr1p associate with higher-molecular-mass protein complexes [8,13]. We tested whether this is the result of direct protein–protein interaction between different hCTR1 molecules by using the yeast two-hybrid system. To study which domains of hCTR1 are involved in this putative interaction, constructs encoding different parts of hCTR1 fused to either the activation domain (plasmid pGADGH) or DNA-binding domain (plasmid pGBT9) of GAL4 were generated. An interaction of the two fusion proteins was detected by analysing the activation of the LacZ and HIS3 reporter genes. As negative controls, we used yeast strains transformed with single vector plasmid plus single fusion construct. The HIS3 and LacZ reporter genes were specifically activated in yeast cells expressing both fusion constructs encoding the N-terminus of hCTR1 (Figures 5A and 5C). No activation was seen with fusion constructs encoding the cytosolic loop between the first two transmembrane domains, or with fusion constructs encoding the C-terminal tail of hCTR1. All transformants were able to grow on plates lacking leucine and tryptophan, showing that the yeast strains contained both introduced plasmids.

Next, we investigated whether this interaction of the N-terminus of hCTR1 was conserved between different species. Therefore the yeast two-hybrid assay was performed with fusion

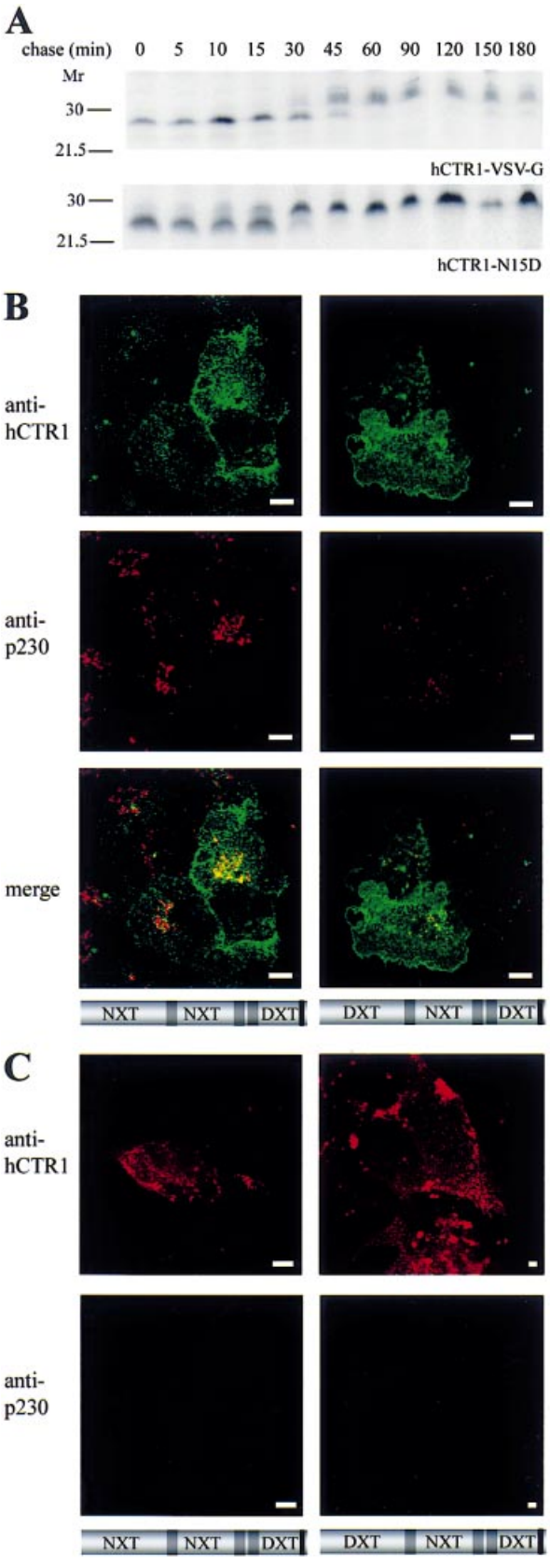

Figure 4 Effect of mutation N15D on hCTR1 biosynthesis and subcellular localization

(**A**) Effect of N15D on hCTR1 biosynthesis. H441 cells were transiently transfected with VSV-G-tagged hCTR1 containing no mutations, or mutation N15D. Cells were pulse-labelled with Tran[^{35}S]^{TM} for 10 min and chased for the indicated time periods with unlabelled methionine. Immunoprecipitation was performed with anti-VSV-G, and proteins were separated by SDS/PAGE followed by fluorography. Molecular-mass markers are indicated on the left. (**B**) Effect of N15D on subcellular localization of hCTR1. H441 cells were transiently transfected with hCTR1-VSV-G or hCTR1-N15D. After permeabilization with Triton X-100, cells were analysed by double-label indirect immunofluorescence, using anti-hCTR1 followed by FITC-conjugated donkey anti-rabbit IgG, and anti-p230 visualized with Cy3-conjugated donkey anti-mouse IgG. Overlap in staining patterns is depicted in yellow in the merged images. (**C**) Effect of N15D on cell surface exposure of hCTR1. Double-label indirect immunofluorescence performed on non-permeabilized transfected H441 cells. Cells were incubated with anti-hCTR1, visualized by Cy3-conjugated donkey anti-rabbit IgG, and anti-p230 visualized by FITC-conjugated donkey anti-mouse IgG. Scale bars, 10 μm. NXT and DXT represent one-letter amino acid code.

constructs encoding the N-terminal tails of mouse, rat and yeast CTR1. As shown in Figure 5(B), all cloned CTR1 N-terminal fragments showed activation of the HIS3 and LacZ reporter genes, indicating that interaction of the N-terminus of CTR1 with itself is conserved between species. No interaction of the N-terminus of hCTR2 with itself (Figure 5B) or in combination with the N-terminus of hCTR1 was detected (results not shown). No growth on plates lacking histidine, leucine and tryptophan was detected in yeast transformed with single fusion construct and single empty vector (Figure 5C), indicating that the detected interactions were specific.

To test whether these interactions are dependent on copper, transformed yeast strains were grown in the presence of the copper chelator BCS before quantification of the strength of the interaction [21]. As a positive control for a copper-dependent interaction, a fusion construct encoding the first four metal-binding domains of ATP7B in combination with a fusion construct encoding full-length hATOX1 were used. Figure 6(A) shows that, consistent with previous findings [26], hATOX1 interacted with the N-terminal domain of ATP7B, and that this interaction was almost completely abolished by the presence of 3 mM BCS in the growth medium. In constrast, BCS had no significant effect on the strength of the interactions between the two N-terminal tails of human, mouse, rat or yeast CTR1, suggesting that copper was not required for these interactions in a similar fashion to the interaction of ATP7B and hATOX1.

To identify domains that are essential for self-interaction of the N-terminus of hCTR1, deletion constructs were generated (Figure 6B). Yeast transformed with hCTR1(18–70) or hCTR1 (40–70) showed a drastic reduction in β-galactosidase activity compared with yeast transformed with plasmids encoding amino acids 1–70 of the N-terminus of hCTR1 (hCTR1-N; Figure 6C). Yeast transformed with hCTR1(1–39) grew very slowly on plates lacking leucine, tryptophan and histidine. Therefore, hCTR1 (1–39)-transformed yeast was cultured in medium lacking leucine and tryptophan. No β-galactosidase activity was detected.

DISCUSSION

The data in this study provide experimental evidence for the topology of hCTR1. In the absence of X-ray crystallograpic data for this integral membrane protein, we have used two approaches to characterize the membrane topology of hCTR1. Both approaches revealed that the N-terminus of hCTR1 is localized outside the cell. In contrast, the amino acids between the first and second hydrophobic domain, as well as the C-terminus of hCTR1, are localized in the cytosol. These results also directly imply that hCTR1 contains three transmembrane domains. Our results are in accordance with another study describing the topology of hCTR1, which was published during the preparation of this manuscript [16]. A similar topology was recently proposed for yCtr1p, based on protease shaving experiments [27]. The topology of CTR1 proteins is therefore conserved between different species.

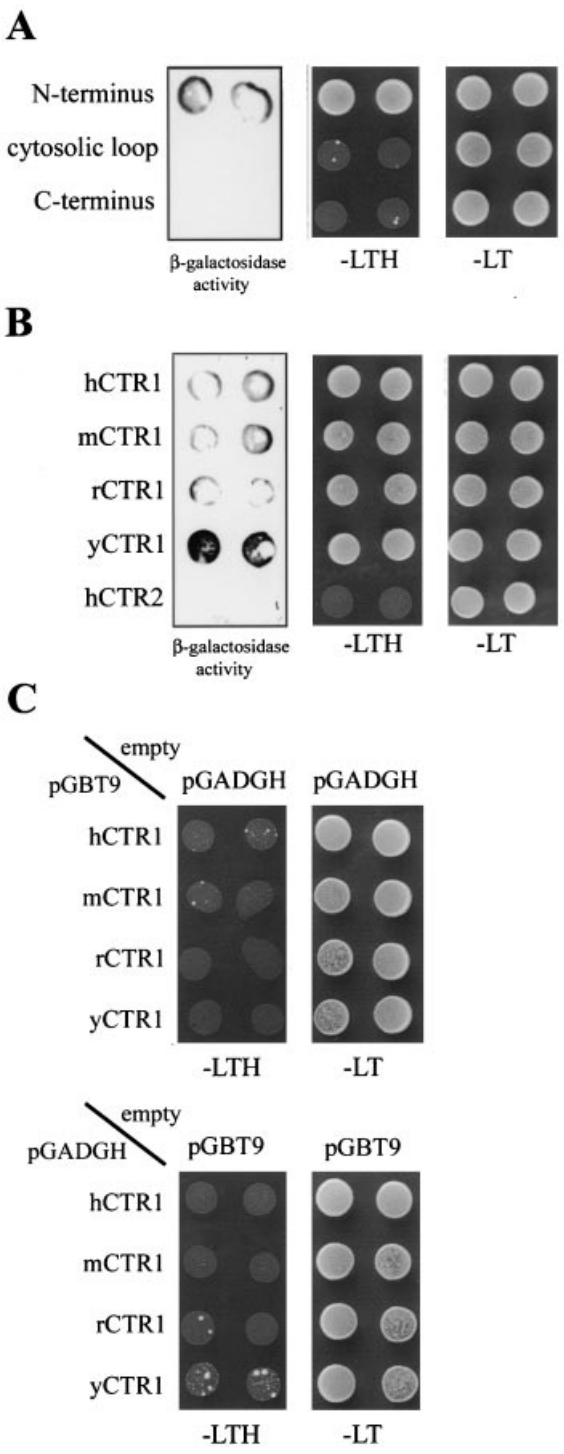

Figure 5 Protein–protein interaction of hCTR1

(**A**) Mapping hCTR1 domain involved in self-interaction. YGH1 cells were co-transformed with pGBT9 and pGADGH fusion plasmids, both encoding either the N-terminus, the cytosolic loop or the C-terminus of hCTR1, fused to the DNA-binding or activation domains of GAL4. Activation of the HIS3 and LacZ reporter genes was assayed on plates lacking leucine, tryptophan and histidine (−LTH). As a control, transformed yeast strains were replica-plated on plates lacking leucine and tryptophan (−LT). (**B**) Species conservation of hCTR1 self-interaction. YGH1 cells were co-transformed with fusion constructs encoding the N-terminal tails of human (h), mouse (m), rat (r) or yeast (y) CTR1, or the N-terminal tail of hCTR2. Activation of the HIS3 and LacZ reporter genes was assayed. (**C**) Specificity of interactions. YGH1 cells co-transformed with single fusion construct and single empty vector as indicated were replica-plated on −LT or −LTH plates. All experiments were performed in duplicate.

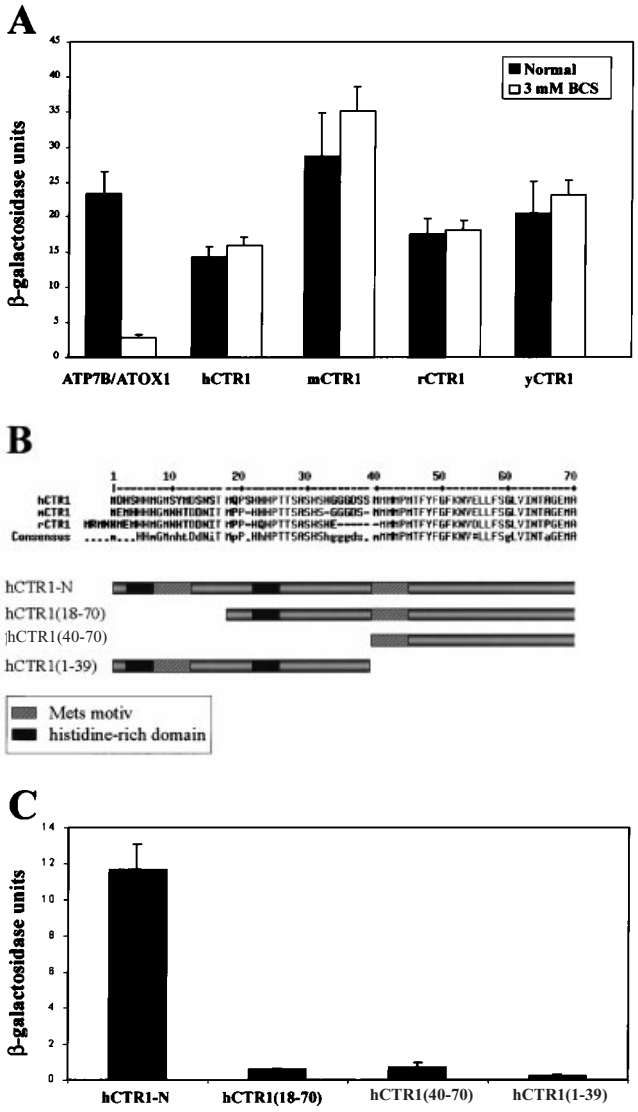

Figure 6 Fine-mapping of the CTR1–CTR1 interaction

(**A**) Copper-dependence of CTR1–CTR1 interaction. YGH1 cells were co-transformed with pGBT9- and pGADGH-based plasmids containing the indicated CTR1 N-terminal domains, and grown in the presence or absence (normal) of 3 mM BCS, a copper chelator. β-Galactosidase activity was measured using ONPG as a substrate [21]. As a control, a fusion construct encoding the first four metal-binding domains of ATP7B in combination with a fusion construct encoding full-length hATOX1 was used. Data are shown as the means ± S.D. from five independent experiments. (**B**) Deletion constructs used for fine mapping of the interaction domain. Alignment of the amino acid sequences of the N-terminal tails of human, mouse and rat CTR1. Schematic representation of constructs encoding amino acids 1–70 of hCTR1 (hCTR1-N), or deletion mutants of hCTR1. Mets motifs are indicated with hatched boxes; histidine-rich domains with black boxes. (**C**) Fine mapping of the interaction domain. YGH1 cells were co-transformed with pGBT9- and pGADGH-based plasmids containing the indicated hCTR1 deletion mutants. β-Galactosidase activity was measured using ONPG as a substrate [21]. Data are shown as the means ± S.D. from five independent experiments.

We also present evidence that CTR1 interacts with itself at the site of its N-terminal domain, which could lead to a system spanning the membrane at least six times. These findings are integrated in the hCTR1 structural model depicted in Figure 7; the structure would be consistent with its proposed role as a copper transporter. The implications of this model are discussed below.

In this model (Figure 7), the single hCTR1 N-linked oligosaccharide is added to the N-terminal region of hCTR1, specifically to residue N15. This N-linked glycosylation site is conserved between human, rat and mouse CTR1 proteins, suggesting that it might be important. N-linked glycosylation is a major form of co-translational modification in eukaryotic protein synthesis, but has variable functional relevance [28]. In some cases, N-glycosylation is necessary for proper intracellular transport of proteins. For instance, lack of glycosylation in the α subunit of the insulin receptor [29,30], CD4 [31] and the angiotensin receptor [32] dramatically impaired targeting of proteins to the cell surface and resulted in intracellular trapping of partially unglycosylated proteins. Our data reveal that hCTR1 without N-linked oligosaccharide matured faster than wild-type hCTR1, which can be explained by the fact that maturation of wild-type hCTR1 was most probably delayed by the glycosylation machinery. No significant impact of removal of the N-linked oligosaccharide chain on the half-life time and cell-surface exposure of hCTR1 was detected. Consistent with these findings, Eisses and Kaplan [16] showed that the absence or presence of the N-linked oligosaccharide has no detectable effect on the copper-transport function of hCTR1.

The structural model places the N-terminal region of hCTR1 in the extracellular environment. This region contains two domains enriched with histidine residues, and two Mets motifs, containing several methionines arranged as Met-Xaa-Met or Met-Xaa-Xaa-Met. These methionine and histidine residues have been postulated to serve as copper ligands [2,6,11]. In contrast to hCTR1, yCtr1p contains eight Mets motifs. Experiments with cells expressing yCtr1p with a deletion of the first 126 amino acid residues spanning all eight Mets motifs show that this part of the N-terminal region of yCtr1p is only essential for the function of the transporter under severe copper-limited conditions [27]. Although experimental evidence that this region binds copper is currently lacking, we propose that the hCTR1 N-terminus is involved in the binding of extracellular copper as an initial step in high-affinity copper import. Upon import, copper is distributed to cellular target enzymes by copper chaperones [1,2]. The mechanisms of copper acquisition by these copper chaperones are unknown, but it was proposed that the exchange of copper between intracellular copper-containing proteins is achieved through direct protein–protein interactions [33]. If a direct interaction between cytoplasmic copper chaperones and hCTR1 exists, this must be mediated, according to the structural model (Figure 7), by the cytosolic loop or the C-terminal domain of hCTR1. However, yeast two-hybrid studies showed that neither domain interacted with the full-length cytosolic copper chaperones hATOX1, hCCS or hCOX17 (results not shown), indicating that other proteins may be involved in this process. Currently we are undertaking yeast two-hybrid library screens to elucidate this missing link.

Many metal transporters, for instance the human zinc importers hZIP1, hZIP2 and hZIP3 [34], the yeast high-affinity zinc transporter ZRT1 [35] and the low-affinity Fe(II) transporter FET4 in *S. cerevisiae* [36], contain between six and eight putative transmembrane domains. Previous studies have also shown that epitope-tagged yCtr1p, yCtr3p and hCTR1 form high-molecular-mass protein complexes [8,13,37]. Taken together with recent genetic studies [27], these data were interpreted as evidence in favour of the hypothesis that CTR1 proteins exist as homodimers or higher-molecular-mass oligomers. These studies [8,13,37] did not address directly whether CTR1 associated with itself and therefore left open the possibility that CTR1 exists as a protein complex with other, currently undefined, proteins. Consistent with the latter possibility, high-affinity copper uptake in *Schizosaccharomyces pombe* is carried out by a hetero-oligomeric complex formed by Ctr4p and Ctr5p, and possibly other proteins [38]. To address this question we used the yeast two-hybrid system to directly assess whether CTR1 could interact with itself. Using this approach we were able to separately express the different domains of CTR1 and determine which domains are involved in this putative interaction. The C-terminal tail and the intracellular loop of hCTR1 did not show interaction in this system. In contrast, the N-terminal domains of human, rat, mouse and yeast CTR1, but not of human CTR2, specifically interacted with itself. The N-terminal domain of hCTR2 did not interact with the N-terminus of hCTR1, which suggests that there is no hetero-oligomerization between these two proteins.

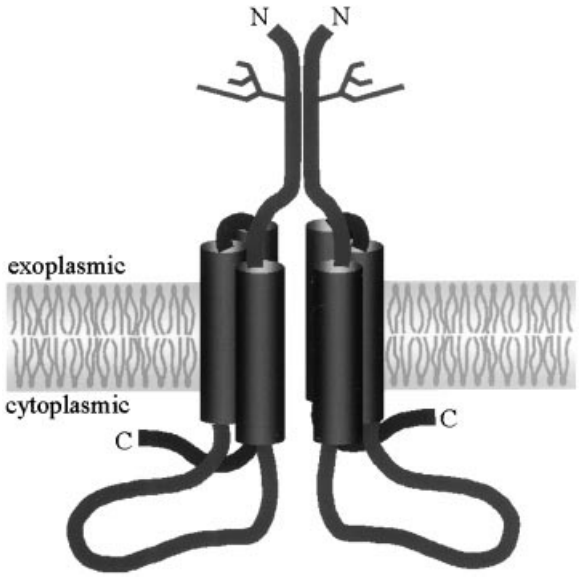

Figure 7 Model of hCTR1 topology

Based on indirect immunofluorescence and a glycosylation mapping strategy, we predict that the N-terminus of hCTR1 is oriented towards the extracellular space, whereas the C-terminus is cytosolic. The N-linked oligosaccharide located at N15 is indicated. We further conclude that hCTR1 spans the plasma membrane three times. The N-terminal tail of hCTR1 directly interacts with itself in a copper-independent manner, leading to a complex spanning the membrane at least six times.

To determine whether the Mets motifs are important for self-interaction of the N-terminus of hCTR1, deletion mutants were generated, lacking either the first or the second Mets motif. Our data suggest that the regions containing both Mets motifs are essential for self-interaction. This finding is consistent with the hypothesis put forward by Wernimont et al. [39], who propose that the methionine loop of the copper-resistance protein PcoC of *Escherichia coli* interacts with another methionine-rich domain. Thus, despite marked sequence differences, which are especially prominent between yeast and mammalian CTR1 proteins (the N-terminus of hCTR1 is only 68 amino acid residues, whereas yCtr1 N-terminus contains 151 amino acid residues), our data suggest common molecular mechanisms of CTR1 self-interaction which are not dependent on copper availability. Since in the yeast two-hybrid studies the fusion proteins are expressed in the cytosol, we conclude that N-linked glycosylation is also not essential for interaction of the hCTR1 N-terminal fragment with itself. Our data do not address the stoichiometry or biochemical mechanisms of these interactions. They also do not exclude the possibility that domains other than the

N-terminus could be involved in interaction of CTR1 with itself *in vivo*. There are some indications that two cysteine residues at the C-terminal end of hCTR1 are involved in stabilizing hCTR1 oligomerization [16]. However, neither of the these cysteines is conserved in other non-mammalian CTR1 proteins, and they are not essential for copper transport activity of hCTR1.

In conclusion, these data provide supporting evidence for the existence of CTR1, but not CTR2, as a homodimer or homo-oligomer. The association is copper-independent, conserved across different species and present in the extracellular N-terminal domain. The data suggest that CTR1 homo-oligomers span the membrane at least six times, thereby permitting the formation of aqueous channels, which could mediate high-affinity copper import.

We are grateful to Dr J. Leusen (Immunotherapy Laboratory, University Medical Center Utrecht, Utrecht, The Netherlands) for help with the yeast two-hybrid system, Dr J. Fransen (Department of Cell Biology, University of Nijmegen, Nijmegen, The Netherlands) for antibodies, Dr G. Posthuma (Department of Cell Biology, University Medical Center Utrecht) for help with confocal microscopy and Ms S. van Mil (Department of Pediatric Gastroenterology, University Medical Center Utrecht) for critical evaluation of this manuscript. This work was supported by grant 902-23-252 from the Dutch Organization for Scientific Research (NWO).

REFERENCES

1 Culotta, V. C. and Gitlin, J. D. (2001) Disorders of copper transport. In The Metabolic and Molecular Basis of Inherited Disease (Scriver, C. R., Beaudet, A. L., Sly, W. S. and Valle, D., eds.), pp. 3105–3126, McGraw-Hill, New York
2 Puig, S. and Thiele, D. (2002) Molecular mechanisms of copper uptake and distribution. Curr. Opin. Chem. Biol. **6**, 171–180
3 Halliwell, B. (1991) Reactive oxygen species in living systems: source, biochemistry, and role in human disease. Am. J. Med. **91**, 14S–22S
4 Valentine, J. S. and Gralla, E. B. (1997) Delivering copper inside yeast and human cells. Science **278**, 817–818
5 Himelblau, E. and Amasino, R. M. (2000) Delivering copper within plant cells. Curr. Opin. Plant Biol. **3**, 205–210
6 Dancis, A., Yuan, D. S., Haile, D., Askwith, C., Eide, D., Moehle, C., Kaplan, J. and Klausner, R. D. (1994) Molecular characterization of a copper transport protein in *S. cerevisiae*: an unexpected role for copper in iron transport. Cell (Cambridge, Mass.) **76**, 393–402
7 Knight, S. A., Labbe, S., Kwon, L. F., Kosman, D. J. and Thiele, D. J. (1996) A widespread transposable element masks expression of a yeast copper transport gene. Genes Dev. **10**, 1917–1929
8 Dancis, A., Haile, D., Yuan, D. S. and Klausner, R. D. (1994) The *Saccharomyces cerevisiae* copper transport protein (Ctr1p). Biochemical characterization, regulation by copper, and physiologic role in copper uptake. J. Biol. Chem. **269**, 25660–25667
9 Ooi, C. E., Rabinovich, E., Dancis, A., Bonifacino, J. S. and Klausner, R. D. (1996) Copper-dependent degradation of the Saccharomyces cerevisiae plasma membrane copper transporter Ctr1p in the apparent absence of endocytosis. EMBO J. **15**, 3515–3523
10 Yonkovich, J., McKenndry, R., Shi, X. and Zhu, Z. (2002) Copper ion-sensing transcription factor Mac1p post-translationally controls the degradation of its target gene product Ctr1p. J. Biol. Chem. **277**, 23981–23984
11 Zhou, B. and Gitschier, J. (1997) hCTR1: a human gene for copper uptake identified by complementation in yeast. Proc. Natl. Acad. Sci. U.S.A. **94**, 7481–7486
12 Klomp, A. E. M., Tops, B. B. J., van den Berg, I. E. T., Berger, R. and Klomp, L. W. J. (2002) Biochemical characterization and subcellular localization of human copper transporter 1 (hCTR1). Biochem. J. **364**, 497–505
13 Lee, J., Peña, M. M. O., Nose, Y. and Thiele, D. J. (2002) Biochemical characterization of the human copper transporter Ctr1. J. Biol. Chem. **277**, 4380–4387
14 Lee, J., Prohaska, J. R. and Thiele, D. J. (2001) Essential role for mammalian copper transporter Ctr1 in copper homeostasis and embryonic development. Proc. Natl. Acad. Sci. U.S.A. **98**, 6842–6847
15 Møller, L. B., Petersen, C., Lund, C. and Horn, N. (2000) Characterization of the *hCTR1* gene: genomic organization, functional expression, and identification of a highly homologous processed gene. Gene **257**, 13–22
16 Eisses, J. F. and Kaplan, J. H. (2002) Molecular characterization of hCTR1, the human copper uptake protein. J. Biol. Chem. **277**, 29162–29171
17 Kuo, Y. M., Zhou, B., Cosco, D. and Gitschier, J. (2001) The copper transporter CTR1 provides an essential function in mammalian embryonic development. Proc. Natl. Acad. Sci. U.S.A. **98**, 6836–6841
18 Lee, J., Prohaska, J. R., Dagenais, S. L., Glover, T. W. and Thiele, D. J. (2000) Isolation of a murine copper transporter gene, tissue specific expression and functional complementation of a yeast copper transport mutant. Gene **254**, 87–96
19 Klomp, L. W. J., Lin, S.-J., Yuan, D. S., Klausner, R. D., Culotta, V. C. and Gitlin, J. D. (1997) Identification and functional expression of HAH1, a novel human gene involved in copper homeostasis. J. Biol. Chem. **272**, 9221–9226
20 Yamaguchi, Y., Heiny, M. E. and Gitlin, J. D. (1993) Isolation and characterization of a human liver cDNA as a candidate gene for Wilson disease. Biochem. Biophys. Res. Commun. **197**, 271–277
21 Guarente, L. (1983) Yeast promoters and lacZ fusions designed to study expression of cloned genes in yeast. Methods Enzymol. **101**, 181–191
22 Kyte, J. and Doolittle, R. F. (1982) A simple method for displaying the hydropathic character of a protein. J. Mol. Biol. **157**, 105–132
23 Ott, C. M. and Lingappa, V. R. (2002) Integral membrane protein biosynthesis: why topology is hard to predict. J. Cell Sci. **115**, 2003–2009
24 Kuo, S. C. and Lampen, O. (1976) Tunicamycin inhibition of (3H) glucosamine incorporation into yeast glycoproteins: binding of tunicamycin and interaction with phospholipids. Arch. Biochem. Biophys. **172**, 574–581
25 Nilsson, I. M. and von Heijne, G. (1993) Determination of the distance between the oligosaccharyltransferase active site and the endoplasmic reticulum membrane. J. Biol. Chem. **268**, 5798–5801
26 Larin, D., Mekios, C., Das, K., Ross, B., Yang, A. and Gilliam, T. C. (1999) Characterization of the interaction between the Wilson and Menkes disease proteins and the cytoplasmic copper chaperone, HAH1p. J. Biol. Chem. **274**, 28497–28504
27 Puig, S., Lee, J., Lau, M. and Thiele, D. J. (2002) Biochemical and genetic analyses of yeast and human high-affinity copper transporters suggest a conserved mechanism for copper uptake. J. Biol. Chem. **277**, 26021–26030
28 Helenius, A. and Aebi, M. (2001) Intracellular functions of N-linked glycans. Science **291**, 2364–2369
29 Bastian, W., Zhu, J., Way, B., Lockwood, D. and Livingston, J. (1993) Glycosylation of Asn397 or Asn418 is required for normal insulin receptor biosynthesis and processing. Diabetes **42**, 966–974
30 Asano, T., Takata, K., Katagiri, H., Ishihara, H., Inukai, K., Anai, M., Hirano, H., Yazaki, Y. and Oka, Y. (1993) The role of N-glycosylation in the targeting and stability of GLUT1 glucose transporter. FEBS Lett. **324**, 258–261
31 Tifft, C. J., Proia, R. L. and Camerini-Otero, R. D. (1992) The folding and cell surface expression of CD4 requires glycosylation. J. Biol. Chem. **267**, 3268–3273
32 Deslauriers, B., Ponce, C., Lombard, C., Larguier, R., Bonnafous, J. C. and Marie, J. (1999) N-glycosylation requirements for the AT1a angiotensin II receptor delivery to the plasma membrane. Biochem. J. **339**, 397–405
33 Rae, T. D., Schmidt, P. J., Pufahl, R. A., Culotta, V. C. and O'Halloran, T. V. (1999) Undetectable free copper: the requirement of a copper chaperone for superoxide dismutase. Science **284**, 805–808
34 Gaither, L. A. and Eide, D. J. (2000) Functional expression of the juman hZIP2 zinc transporter. J. Biol. Chem. **275**, 5560–5564
35 Zhao, H. and Eide, D. (1996) The yeast ZRT1 gene encodes the zinc transporter protein of a high-affinity uptake system induced by zinc limitation. Proc. Natl. Acad. Sci. U.S.A. **93**, 2443–2458
36 Dix, D. R., Bridgham, J. T., Broderius, M. A., Byersdorfer, C. A. and Eide, D. J. (1994) The FET4 gene encodes the low affinity Fe(II) transport protein of *Saccharomyces cerevisiae*. J. Biol. Chem. **269**, 26092–26099
37 Peña, M. M. O., Puig, S. and Thiele, D. J. (2000) Characterization of the *Saccharomyces cerevisiae* high affinity copper transporter Ctr3. J. Biol. Chem. **275**, 33244–33251
38 Zhou, H. and Thiele, D. J. (2001) Identification of a novel high affinity copper transport complex in the fission yeast *Schizosaccharomyces pombe*. J. Biol. Chem. **276**, 20529–20535
39 Wernimont, A. K., Huffman, D. L., Finney, L. A., Demeler, B., O'Halloran, T. V. and Rosenzweig, A. C. (2002) Crystal structure and dimerization equilibria of PcoC, a methionine-rich copper resistance protein from *Escherichia coli*. J. Biol. Inorg. Chem. **8**, 185–194

Received 17 July 2002/14 November 2002; accepted 5 December 2002
Published as BJ Immediate Publication 5 December 2002, DOI 10.1042/BJ20021128